第36卷，第6期 光 谱 学 与 光 谱 分 析 Vol. 36, No. 6, pp1978-1986
2016年6月 Spectroscopy and Spectral Analysis June, 2016

Retrieval and Analysis of Atmospheric Temperature Using a Rotational Raman Lidar Observation

LIU Yu-li[1,2], XIE Chen-bo[1]*, SHANG Zhen[1],
ZHAO Ming[1], CAO Kai-fa[1], SUN Yue-sheng[2]

1. Key Laboratory of Atmospheric Composition and Optical Radiation, Anhui Institute of Optics and Fine Mechanics, Chinese Academy of Sciences, Hefei 230031, China
2. Department of Physics, Electronic Engineering Institute of PLA, Hefei 230037, China

Abstract Due to the existence of the aerosol, the traditional method of measuring atmospheric temperature by using Rayleigh scattering technique has limitations in the low altitude. A pure rotational Raman lidar to get tropospheric temperature profiles is built. We carried out the atmospheric temperature observation in Beijing for two months. The atmospheric temperature profile was retrieved using the observed rotational Raman scattering signals. The effect of smooth window, calibration range and calibration constant on the retrieval precision of the atmospheric temperature was evaluated and analyzed. The results show that with the increase of smooth window, the mean absolute deviation between the lidar and radiosonde firstly decreases and then increases; in order to remove effectively the effect of random error in the return signals, while maintaining the fine vertical structure of temperature profile, it is better to choose the range between 600 and 1 200 m for smooth window. When calibration range is different, the mean absolute deviation between the lidar and radiosonde is varied, the relative variation of the deviation is about 0.07 K. When both calibration constant a and b increase or decrease, the mean deviation between the lidar and radiosonde increases; when one increases and another decreases, the mean deviation has a tendency to cancel each other out. The variance probability of a or b is not equal, and the variance of a and b is always contrary in the sign; the mean deviation is not sensitive to variance of a or b, and it is sensitive to the whole variance of a and b, about 91.7% of the mean deviation is in the range between −3 and 3 K. These results provide the theoretical basis for the selection of smooth window and calibration range in pure rotational Raman lidar data retrieval, and the reference for the error of actual temperature inversion result caused by lidar calibration constant.

Keywords Lidar; Atmospheric temperature; Calibration constant; Error analysis
中图分类号: TN958.98 **文献标识码**: A **DOI**: 10.3964/j.issn.1000-0593(2016)06-1978-09

Introduction

The atmospheric temperature is an important meteorological parameter in atmospheric physics, weather forecasting and atmospheric environmental research. The meteorological sounding data analysis in recently several years indicated that the temperature in the lower troposphere increased obviously,

Received: 2015-09-16; **accepted**: 2015-12-08
Foundation item: the Open Research Fund of Key Laboratory of Atmospheric Composition and Optical Radiation, Chinese Academy of Sciences (2013JJ01); National Natural Science Foundation of China (41005014, 41205020); China Special Fund for Meteorological Research in the Public Interest (GYHY201206037); the Key Research Program of the Chinese Academy of Sciences (KJZD-EW-TZ-G06-01); the Wanjiang Center for Development of Emerging Industrial Technology (12Z0104074)
Biography: LIU Yu-li, (1979—), Electronic Engineering Institute of PLA, Department of Physics, lecturer
e-mail: 13956989561@139.com *Corresponding author e-mail: cbxie@aiofm.ac.cn

the temperature in the upper troposphere and stratosphere decreased[1]. The change of atmospheric temperature distribution will also result in the changes of atmospheric physical and chemical, dynamic process and the distribution of trace elements. For example, the inversion structure of lower troposphere often inhibits the diffusion of the pollutants under the boundary layer, and causes the increasing concentration of the pollutants. So the temperature profile of troposphere is very important. By using the relationship between spectral line intensity and temperature of the N_2 or O_2 molecules, the rotational Raman lidar can measure the lower altitude atmospheric temperature, and it is hardly affected by aerosols and cirrus clouds[2], which has the highest accuracy and the simplest data processing method among four lidar methods in temperature measurement (pure rotational Raman method[2], Rayleigh method[3], differential absorption method[4], vibrational Raman method[5]). This technique of temperature measurement by a rotational Raman lidar was first proposed by Cooney in 1972[6]. In recent years, rotational Raman lidar technology has developed very quickly, both in domestic[7-9] and overseas[3,10-11]. In this paper, the measurement principle and system structure of pure rotational Raman lidar are briefly introduced. The retrieval results of atmospheric temperature profile are given. Different effects on temperature profile resulting from smooth window, calibration range and calibration constant are analyzed. Temperature inversion analysis provides not only the theoretical basis for choosing the appropriate smooth window and calibration range in pure rotational Raman lidar data retrieval, but the reference for the error of actual temperature inversion result caused by calibration constant.

1　Measurement principle and system structure of pure rotational Raman lidar

1.1　Measurement principle

A 354.7 nm laser pulse is emitted in the atmosphere. The rotational Raman backscattered photon counts of N_2 and O_2 can be expressed as[7]

$$N(z) = \frac{CN_0 T'^2(z)}{z^2} \sum_{i=N_2,O_2} \sum_{J_i} \beta(J_i, T) \qquad (1)$$

Where C is lidar constant, N_0 is photon number of launched laser pulse, $T'(z)$ is atmospheric transmission, z is the detection height, J is the rotational quantum number, T is temperature, β is backscatter coefficient, which can be written as

$$\beta = n(z) \frac{64\pi^2}{45} \nu_l^4 g_I(J) \gamma^2 \frac{2Bhc}{(2I+1)^2 kT} (2J+1) \times \exp\left\{ \frac{Bhc}{kT} \times J(J+1) \left[1 - \frac{D}{B} J(J+1) \right] \right\} | H_{J'}^J |^2 \qquad (2)$$

The implication and constant value related to physical quantities see references 7. According to Eq. (2), the pure rotational Raman spectral relative intensity of N_2 at different temperature is calculated, as shown in Fig. 1. The spectral line intensity corresponding to high and low quantum number changes inconsistently with temperature, so atmospheric temperature can be derived from the return signals ratio of high and low-level quantum numbers of N_2 and O_2 molecules

$$T = \frac{a}{\ln \frac{N_{JL}(z)}{N_{JH}(z)} - b} \qquad (3)$$

Where N_{JL} and N_{JH} are photon counts of low and high-level quantum numbers caused by lidar return signals, a and b are the calibration constants which can be derived by comparing the signal intensity ratio of the lidar with the temperature data obtained simultaneously by a radiosonde.

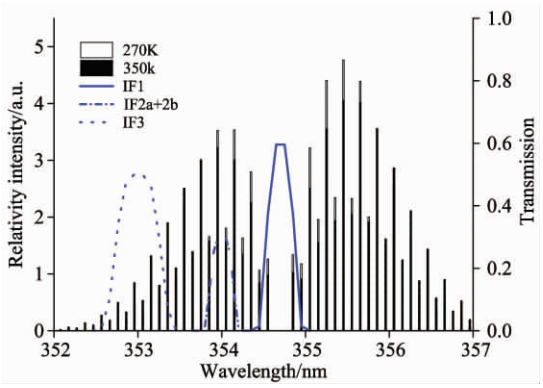

Fig. 1　Rotational Raman scattering spectrum and filter transmission for N_2

1.2　System structure

The lidar structure is shown in Fig. 2. The light source is a Nd∶YAG laser which provides a single pulse output energy of 180 mJ at the wavelength of 354.7 nm and a pulse repetition rate of 20 Hz. The laser is guided into the atmosphere by a steering mirror and the beam expander. The expander can reduce the laser beam divergence to 0.15 mrad. The backscattered light is collected by a Cassegrain telescope with diameter of 450 mm, focal length of 4m and receiving field of view of 1 mrad. After the light goes through an adjustable field stop, a collimating lens and a steering mirror, it is guided into a polychromator box. This box is made up by a series of interference filters. The central wavelengths (CWL) of the filters can be tuned by selecting angles of incidence (AOI). In this box, the light firstly passes the broadband interference filter IF0 with a transmission band of 8 nm full width at half maximum (FWHM), and this filter blocks the atmospheric background light while the elastic and both rotational Raman signals are transmitted. Secondly, the light passes the narrow band interference filter IF1, and this filter extracts elastic scattering signal of 354.7 nm used to detect the aerosol. Thirdly, the

light passes the narrow band interference filter IF2, and this filter extracts rotational Raman scattering signal of 354.0 nm used to detect the temperature. Because the transmission band of IF2 is very close to the laser wavelength, we use two filters in the first rotational Raman channel. Finally, the light passes the narrow band interference filter IF3, and this filter extracts rotational Raman scattering signal of 353.0 nm used to detect the temperature. The data acquisition is performed with a Licel transient recorder. The filter parameters are listed in Table 1, and transmission curve is shown in Fig. 1.

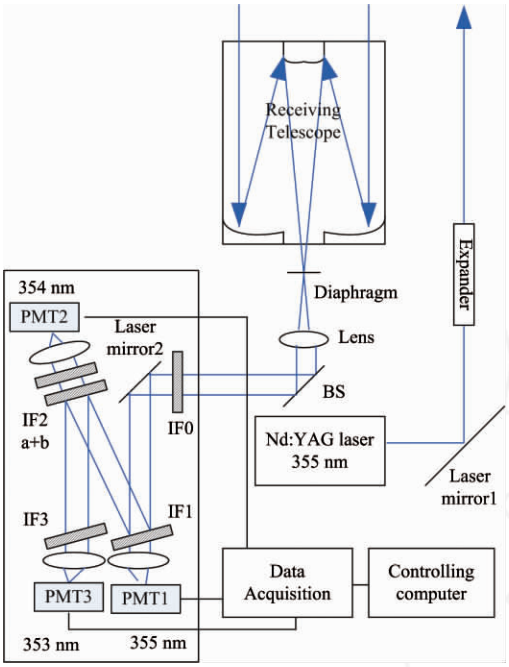

Fig. 2 Diagram of the rotational Raman lidar

Table 1 Filter parameters

	AOI/deg	CWL/nm	FWHM/nm	Peak transmission
IF0	0.0	353.7	8.0	0.5
IF1	5.5	354.7	0.3	0.6
IF2a	6.5	354.0	0.3	0.5
IF2b	6.5	354.0	0.3	0.6
IF3	6.1	353.0	0.5	0.5

2 Results and discussion

The statistical temperature errors can be gotten through Eq. (3) and the error propagation theory[12]

$$\delta T = T\sqrt{\left(\frac{\delta a}{a}\right)^2+\left[\frac{\delta b}{\ln\frac{N_{low}}{N_{high}}-b}\right]^2+\frac{\left(\frac{\delta N_{low}}{N_{low}}\right)^2+\left(\frac{\delta N_{high}}{N_{high}}\right)^2}{\left(\ln\frac{N_{low}}{N_{high}}-b\right)^2}} \tag{4}$$

Where we have assumed that errors in determining calibration constants are zero, Eq. (4) can be simplified to

$$\delta T = T\sqrt{\frac{\left(\frac{\delta N_{low}}{N_{low}}\right)^2+\left(\frac{\delta N_{high}}{N_{high}}\right)^2}{\left(\ln\frac{N_{low}}{N_{high}}-b\right)^2}} \tag{5}$$

The photon counts of rotational Raman backscattered, background light signal and PMT dark counts follow a Poisson distribution. Therefore, the relative uncertainty of cumulative signals is given by $\delta N/N=1/\sqrt{N}$ (N is the number of cumulative photons), and then Eq. (5) can be derived

$$\delta T = \frac{T}{\ln\frac{N_{low}}{N_{high}}-b}\sqrt{\frac{1}{N_{low}}+\frac{1}{N_{high}}} \tag{6}$$

The tropospheric atmospheric temperature observation was conducted on the night of 2nd November 2014, in Beijing. Fig. 3(a) shows a lidar measurement of the temperature profile and the simultaneous temperature profile measured by a radiosonde. Error bars in the figure include statistical temperature error only. Fig. 3(b) shows deviations between the two sensors. The measurement was carried out in a clear atmosphere, and data were acquired for a 3.3 min observation time and a 5 min interval. For the calibration we chose a local radiosonde that was launched at 20:00 on 2 November 2014 in a distance of 30 km to the lidar site. Lidar data, acquired with a vertical resolution of 7.5 m, have been vertically smoothed to a final resolution of 600 m in order to reduce signal fluctuations. As can be seen from the Fig. 3, tropospheric temperature decreases faster with increasing height, the lidar and radiosonde measurements appear to be in good agreement. A statistical temperature error reaches 1 K at height of 4.2 km, and 2 K at height of 7.1 km. Deviations between the two sensors are less than 2 K below 8 km. The lidar measurement results is smaller than radiosonde data below 1 km, which is associated with different overlap functions in the two

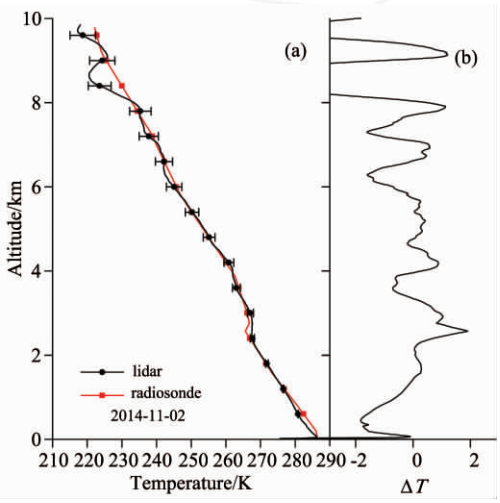

Fig. 3 (a) Temperature profile on 2 November 2014: lidar measurement (solid line) and radiosonde data (dot line); (b) Deviations between lidar and radiosonde

rotational Raman channels and infiltrating aerosol. The lidar measurement of temperature uncertainty is bigger above 8 km, this is because the signal-to-noise ratio (SNR) decreases. This indicates that the lidar measurement of temperature distribution is reliable. To reduce the statistical error, we can increase the number of shots or smooth window.

3 Factors affecting atmosphere temperature profile retrieval

3.1 Smooth window

When the calibration range of 1～7 km remains unchanged, the lidar data are smoothed with a gliding window with an average length of 300～2 000 m. The lidar measurement of temperature profile is more and more close to the radiosonde profile with the increment of smooth window. To a certain degree, the lidar measurement of temperature profile deviates from radiosonde profile at the low-level and high-level, as seen in Fig. 4. This is because when the smooth window is small, the random error in the signals plays a leading role and the inversion temperature fluctuates near the radiosonde measurement value; when the smooth window is big, the random error in the signals is smoothed effectively and the spatial variation characteristics of temperature are also subsequently eliminated, then a system's deviation between the retrieved temperature profile and the radiosonde measurement value appears. With the increase of the smooth window, the mean absolute deviation is smaller and smaller. It is easy to achieve stabilization stage for good signals, while it is difficult to reach stabilization stage for poor signals. After the stabilization stage, the mean absolute deviation begins to increase with the continued increase of smooth window, as seen in Fig. 5. This is because a lidar measurement of the temperature profile deviates from radiosonde data at the low-level and high-level. When smooth window varies from 300 to 900 m, the mean absolute deviation at 20:10 decreases by 0.5 K;

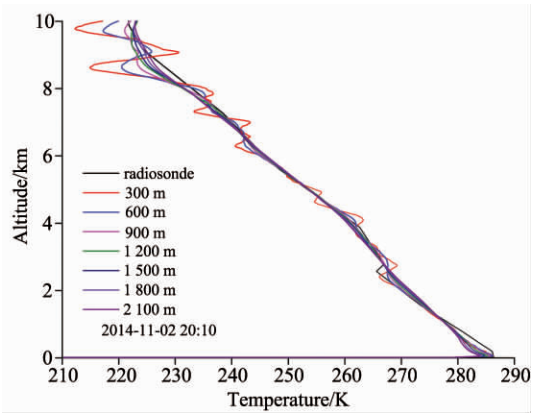

Fig. 4　Temperature profiles under different smooth windows

when smooth window varies from 900 to 2 000 m, the mean absolute deviation increases by 0.4 K. The results show that, to remove effectively the effect of random error in the return signals, while maintaining the vertical structure of temperature profile, it is better to choose the range between 600 and 1 200 m for smooth window, and the signals can't be smoothly unlimitedly. This is the selection range of smooth window when pulse number is 4 000 shots. If the pulse number increases, the smooth window should be appropriate reduced.

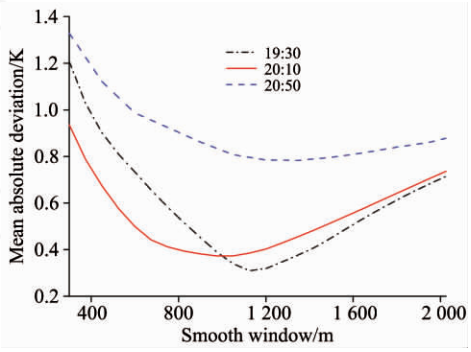

Fig. 5　Mean absolute deviations under different smooth windows

3.2 Calibration range

Because the overlap funcuions in the two rotational Raman channels at low-level are different and the SNR is relatively small at high-level, we choose a middle range to calibrate. The SNR of this range is larger, and the signal is better. If we choose a calibration lowest altitude of 0.5 km and toppest altitude of 6, 7 and 8 km respectively for 20:10 set of data, mean absolute deviation between lidar and radiosonde in the height range between 1 and 8 km is 0.59, 0.53, 0.54 K respectively shown in Fig. 6, so we choose 7 km as the toppest altitude. When the toppest altitude is 7 km, the lowest altitude is 0.5, 1, 2 km respectively, mean absolute deviation in the height range between 1 and 8 km is 0.53, 0.52 and 0.58 K respectively, so we choose 1 km as the lowest altitude. When the calibration range is in the range between 1 and 7 km for this set of data, the mean absolute deviation is the smallest, so choosing 1 to 7 km as the calibration range. Therefore, the calibration constant $a=878.13$, $b=-3.19$ can be obtained. When calibration range is different, the mean absolute deviation between the lidar and radiosonde is varied, the relative variation of the deviation is about 0.07 K.

3.3 Calibration constant

To estimate the influence of calibration constant on the retrieval precision of temperature, we have studied the variance of calibration constant. The radiosonde was launched at 20:00 on 2 November 2014, and a period of data (measurement time during 19:20 to 20:40) which is close in time to

the radiosonde measurement was selected. Under the same smooth window and calibration range, the calibration constant a, relative error of a, the calibration constant b and relative error of b are shown in Table 2.

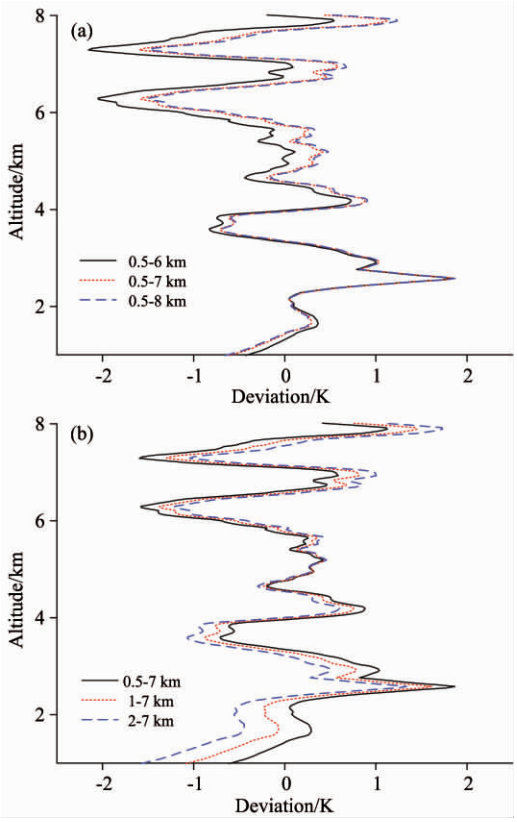

Fig. 6 Deviation profiles under different calibration ranges

Table 2 a, b, and relative error of a and b on November 2, 2014

time	a	relative error/%	b	relative error/%
19:20	916.42	3.5	−3.33	−3.4
19:25	810.51	−8.4	−2.94	8.8
19:30	839.63	−5.1	−3.05	5.5
19:35	877.83	−0.8	−3.18	1.3
19:40	881.65	−0.4	−3.21	0.4
19:45	882.22	−0.3	−3.21	0.6
19:50	845.53	−4.5	−3.08	4.7
19:55	894.45	1.1	−3.26	−1.0
20:00	853.84	−3.5	−3.11	3.5
20:05	862.85	−2.5	−3.14	2.5
20:10	878.26	−0.8	−3.19	1.0
20:15	902.88	2.0	−3.29	−2.0
20:20	926.30	4.7	−3.39	−5.0
20:25	893.81	1.0	−3.26	−1.1
20:30	997.40	12.7	−3.65	−13.1
20:35	859.82	−2.9	−3.14	2.8
20:40	882.38	−0.3	−3.22	0.2

As can be seen from Table 2, the calibration constants of each set of data are changing. This is mostly due to lidar system parameters such as the output laser wavelength, energy and detecting unit performance changing during the observation period, the differences of SNR of the Raman signals within the scope of calibration height, and the differences of measurement values between lidar and radiosonde in time and space during the calibration period. The variance of a is 4.7%, the variance of b is 4.9%. The variances of a and b is all greater than 4%. Next, we analyze the effect of the variance of a, b on temperature profile and the probability of mean deviation falling into the range between −3 and 3 K when both a and b change within 4%. Nine atmospheric temperature profiles are derived when b don't change and a change by 4% with a step length of 1%, and when a don't change and b change by 4% with a step length of 1% as shown in Figs. 7—8. When a increases, the temperature profile moves to the right, and the temperature increases; when b increases, the temperature profile also moves to the right, and the temperature also increases. With the increase of a or b, the mean deviation between the lidar and radiosonde is a linear distribution, and the standard deviation between the lidar and radiosonde is the parabola shape as shown in Figs. 9—10. When a increases to 4%, the mean deviation increases by 10.36 K, and the standard deviation increases by 0.14 K;

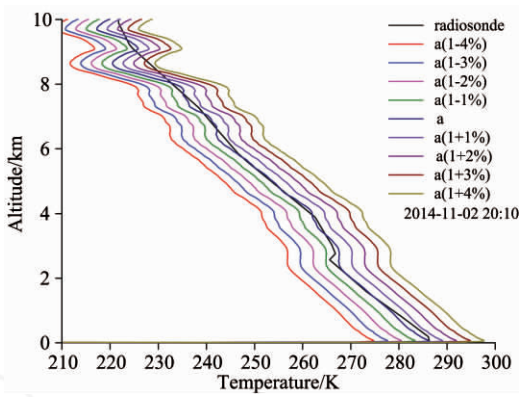

Fig. 7 Temperature profiles with b constant and a variable

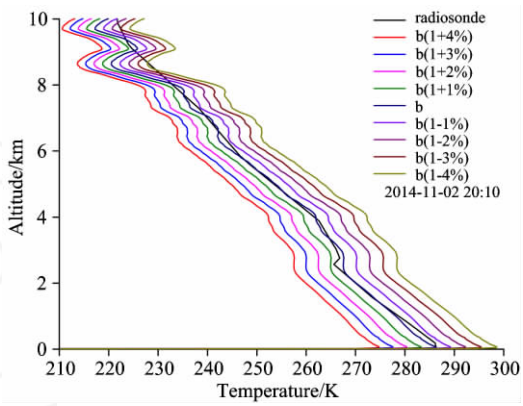

Fig. 8 Temperature profiles with a constant and b variable

when b increases to 4%, the mean deviation increases by 9.43 K, and the standard deviation increases by 0.36 K. The mean deviation caused by the variance of a is greater than b, so the variance of a is more likely to cause the translation of profile. The standard deviation caused by the variance of b is greater than a, so the variance of b is more likely to lead to the change of profile shape.

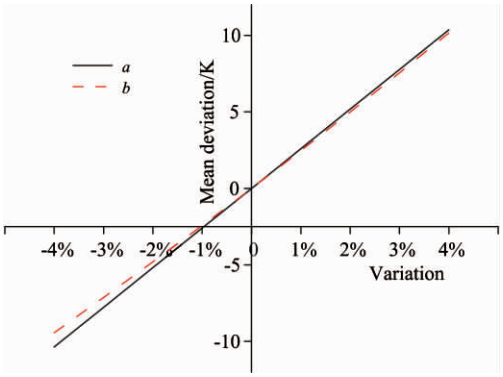

Fig. 9　Mean deviation between the lidar and radiosonde versus a or b

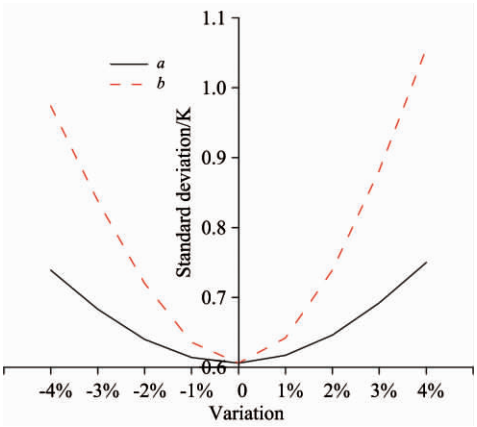

Fig. 10　Standard deviation between the lidar and radiosonde versus a or b

When a changes −4%, −3%, −2%, −1%, 0, 1%, 2%, 3%, 4% and b also changes −4%, −3%, −2%, −1%, 0, 1%, 2%, 3%, 4%, respectively, there are 81 kinds of combinations, and 81 atmospheric temperature profiles are retrieved as shown in Fig. 11. The middle profiles are dense, both profiles are thin. When both a and b increase to 4%, the retrieved temperature profile is the right-most line, and the mean deviation between lidar and radiosonde is about 20.9 K. When both a and b decrease to 4%, the retrieved temperature profile is the left-most line, and the mean deviation is about −19.4 K. When a increases to 4% and b decreases to 4%, or a decreases to 4% and b increases to 4%, the retrieved temperature profile is in the middle position, close to the radiosonde profile, and the mean deviation is about 0.5 K, −0.1 K, respectively. When both a and b increase or decrease, the retrieved temperature profile is away from radiosonde profile, and the deviation is bigger and bigger; When one increases and another decreases, the retrieved temperature profile is close to the radiosonde profile, and the deviation has a tendency to cancel each other out. Fig. 12 shows a ratio between the number of deviations within a certain temperature range and the total number of deviations for the variance within 4% for both a and b. It can be seen that the changing tendency of three different time deviation weight curves are consistent and they are approximately a normal distribution. When both a and b change within 4%, 27% of the mean deviations are in the range between −3 and 3 K. This is a statistical rule when the variance probabilities of a and b are equal. if the variance probabilities of a and b are not equal, and the probability of the mean deviation falling into the range between −3 and 3 K should be multiplied by a weighting factor.

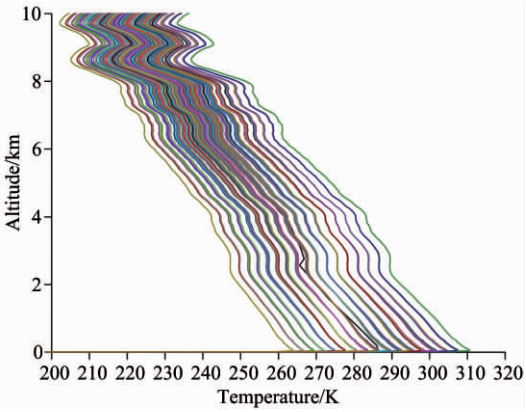

Fig. 11　Temperature profiles for the variance within 4% for both a and b

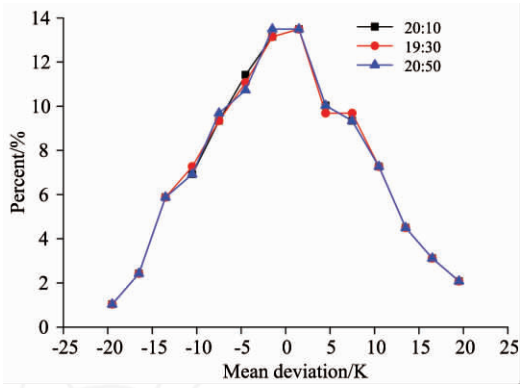

Fig. 12　Ratio between the number of deviations within a certain temperature range and the total number of deviations for the variance within 4% for both a and b

Fig. 13 can be plotted according to Table 2. As can be seen from the Fig. 13, the majority of the variance of a is −3%, and the majority of variance of b is 3%, the variance probabilities of a and b are not equal. It can be seen from Eq.

(4) that the variance of 1% for calibration constant a leads to temperature error of 1%, the variance of 1% for b leads to temperature error range between 1% and 0.85% at altitudes of 1～8 km. By Table 2, you can also see that the variances of a and b are always contrary in sign, a positive and a negative. Through the analysis of the above, we know that the deviation has a tendency to cancel each other out when the variances of a and b are contrary in sign. By the whole variance of a and b, we can see where is the approximate range of mean deviation.

We will apply the 13th calibration constant ($\bar{a}$=865.23, $\bar{b}$=−2.93) to the 16th, 17th and 21th (13, 16, 17, 21th continuous observation, clear weather), the retrieved atmospheric temperature profiles is shown in Fig. 14. Lidar and radiosonde measurements appear to be in good agreement, and they change surround radiosonde profile or deviate a little from the radiosonde profile.

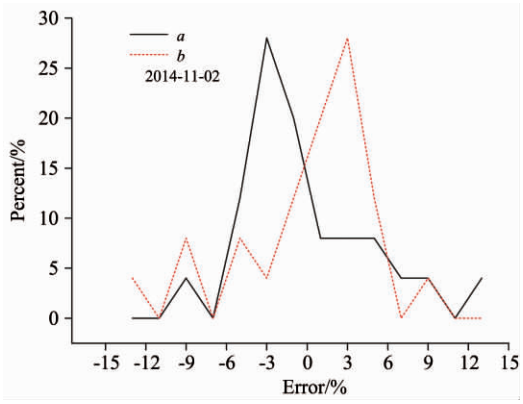

Fig. 13 Ratio between the number of errors within a certain relative error range and the total number of errors for a or b

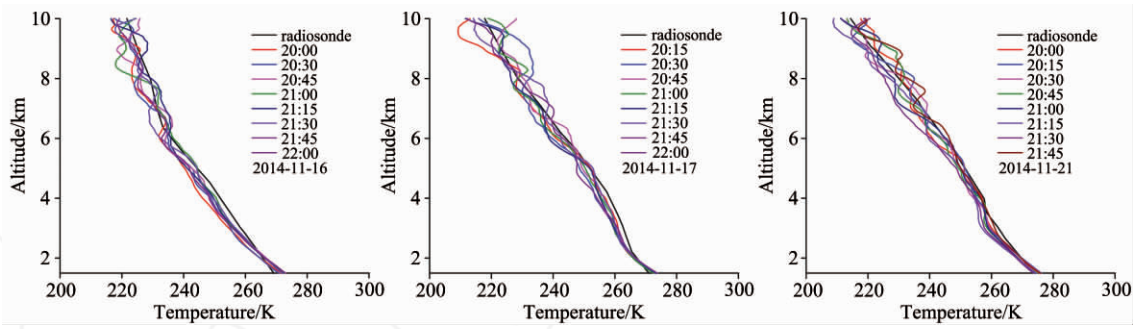

Fig. 14 Retrieved temperature profiles on November 16, 17, 21 using calibration constant on November 13

Under the same smooth window and calibration range, the 16th, 17th and 21th calibration constant a, b, the relative error of a and b which is relative to the 13th calibration constant, retrieved the mean deviation between the lidar and radiosonde using the 13th calibration constant are shown in Tables 3—5.

Table 3 a, b, relative error of a and b, and mean deviation on 16 November 2014

time	a	relative error/%	b	relative error/%	mean deviation/K
20:00	919.53	6.3	−3.11	−6.1	−3.05
20:30	908.31	5.0	−3.07	−4.8	−2.47
20:45	911.85	5.4	−3.10	−5.8	−1.31
21:00	845.09	−2.3	−2.85	2.7	−0.25
21:15	841.18	−2.8	−2.83	3.4	−0.58
21:30	923.05	6.7	−3.15	−7.5	−1.34
21:45	935.74	8.1	−3.19	−8.9	−1.98
22:00	877.16	1.4	−2.97	−1.4	−0.68

As shown in Tables 3—5, both the variance of a and b may be very large, but no matter how large the variance of a or b is, their whole variance is basically in the range between −1% and 1%, so the mean deviation is essentially in the range between −3 and 3 K. Through data analysis for 16, 17, 21 November, about 91.7% of mean deviations are in the range between −3 and 3 K by calculation. The statistical regularity is right under the continuous observation, clear atmosphere and the same calibration range. If the calibration range is different, or light path adjusts, or the sky has cloud, the statistical regularity is not established.

Table 4 a, b, relative error of a and b, and mean deviation on 17 November 2014

time	a	relative error/%	b	relative error/%	mean deviation/K
20:15	933.88	7.9	−3.18	−8.5	−1.66
20:30	937.59	8.4	−3.18	−8.5	−2.80
20:45	847.09	−2.1	−2.85	2.7	−1.05
21:00	913.75	5.6	−3.10	−5.8	−1.64
21:15	923.65	6.8	−3.13	−6.8	−2.18
21:30	797.42	−7.8	−2.66	9.2	−0.33
21:45	840.90	−2.8	−2.82	3.8	−1.39
22:00	833.47	−3.7	−2.78	5.1	−1.55

Table 5　a, b, relative error of a and b, and mean deviation on 21 November 2014

time	a	relative error/%	b	relative error/%	mean deviation/K
20:00	926.74	7.1	−3.16	−7.8	−1.38
20:15	870.05	0.6	−2.94	−0.3	−0.67
20:30	845.97	−2.2	−2.84	3.1	−0.92
20:45	903.85	4.5	−3.06	−4.4	−1.95
21:00	945.97	9.3	−3.23	−10.2	−1.84
21:15	892.13	3.1	−3.00	−2.4	−2.52
21:30	1021.97	18.1	−3.50	−19.5	−3.98
21:45	830.86	−4.0	−2.80	4.4	−0.06

4　Conclusions

The atmospheric temperature profile was retrieved by pure rotational Raman backscattering return signals. The statistical error is smaller than1K below 4.2 km and 2 K below 7.1 km, and deviations between the lidar and radiosonde are less than 2 K below 8 km with a laser energy of 180 mJ, averaged pulse number of 4 000 and smooth window of 600 m. The retrieval results of the atmospheric temperature are associated with smooth window, calibration range and calibration constant. When smooth window varies from 300 to 2 000 m, the mean absolute deviation between the lidar and radiosonde firstly decreases by 0.5 K and then increases by 0.4 K, so the smooth window can only choose values between a certain range. The calibration range of 1～7 km is chosen according to the smallest mean absolute deviation. Variance of calibration constant a or b leads to not only the translation of temperature profile, but the change of temperature profile shape, and the effect of b on profile shape is larger than a; When both a and b increase or decrease, the mean deviation between the lidar and radiosonde increases; when one increases and another decreases, the mean deviation has a tendency to cancel each other out. When the variance probabilities of a and b are equal and both a and b change within 4%, 27% of the mean deviation are in the range between −3 and 3 K. In fact the variance probability of a or b is not equal, their whole variance basically tends to the range between −1% and 1%, and about 91.7% of the mean deviations are in the range between −3 and 3 K. The analysis of these errors can be used as references for the selection of smooth window, calibration range and the error of actual temperature inversion results caused by lidar calibration constant.

References

[1] Ding Yi-hui. China's Climate Change: Science, Impact, Orientation and Countermeasures Study. Beijing: China Environmental Science Press, 2009.
[2] Achtert P, Khaplanov M, Khosrawi F, et al. Atmos. Meas. Tech., 2013, 6: 91.
[3] Chen W N, Tsao C C, Nee J B. Journal of Atmospheric and Solar-Terrestrial Physics, 2004, 66: 39.
[4] Korb C L, Weng C Y. Appl. Opt., 1983, 22: 3759.
[5] Wu Yong-hua, Li Tao, Zhou Jun. Chinese Journal of Atmospheric Sciences, 2002, 26(5): 702.
[6] Cooney J A. J. Appl. Meteorol., 1972, 11(1): 108.
[7] Jia Jing-yu, Yi Fan. Appl. Opt., 2014, 53(24): 5330.
[8] Chen S, Qiu Z, Zhang Y, et al. J. Quant. Spectrosc. Radiat. Transfer., 2011, 112: 304.
[9] Mao J D, Xie Zh, Wu M, et al. Proceedings of the SPIE, 2008, 7130: 1.
[10] Imaki M, Kawai H, Kato T, et al. Japanese Journal of Applied Physics, 2012, 51(4): 052401.
[11] Hammann E, Behrendt A, Mounier F L. Atmospheric Chemistry and Physics, 2015, 15(3): 2867.
[12] Russell P B, Swissler T J, McCormick M P. Appl. Opt., 1979, 18(22): 3783.

基于纯转动拉曼谱线激光雷达的大气温度反演分析

刘玉丽[1,2]，谢晨波[1*]，尚 震[1]，赵 明[1]，曹开法[1]，孙越胜[2]

1. 中国科学院安徽光学精密机械研究所大气成分与光学重点实验室，安徽 合肥 230031
2. 解放军电子工程学院物理教研室，安徽 合肥 230037

摘 要 由于气溶胶的影响，传统的瑞利散射法测量低空大气温度有一定的局限，为此开展了纯转动拉曼法测量低空大气温度。利用纯转动拉曼激光雷达在北京进行了 2 个月的大气温度观测，由观测数据反演了温度廓线。在基于 N_2 和 O_2 的纯转动拉曼谱线特征进行大气温度反演过程中，分析了平滑窗口、定标范围和定标常数对温度反演精度的影响。结果显示随着平滑窗口的增大，雷达和无线电探空仪测量的温度之间的平均绝对偏差先减小后增加，为有效去除信号中随机误差的影响，同时保留温度廓线的垂直结构，平滑窗口应选择 600～1 200 m 比较好。定标范围不同，雷达和无线电探空仪测量的温度之间的平均绝对偏差就不同，相对变化约为 0.07 K。当定标常数 a，b 都增大或都减小时，雷达和无线电探空仪测量的温度之间的平均偏差增大，当一个增大另一个减小时，平均偏差相互抵消；a，b 的变化不是等几率的，在符号上总是相反的；平均偏差对 a 的变化不敏感，对 b 的变化也不敏感，对 a 与 b 的整体变化敏感，约 91.7%平均偏差落入 －3～3 K 之间。该研究分析结果对纯转动拉曼激光雷达数据反演中涉及的平滑窗口、定标范围的选择提供了理论依据，对激光雷达定标常数造成实际温度反演结果的误差提供了参考。

关键词 激光雷达；大气温度；定标常数；误差分析

（收稿日期：2015-09-16，修订日期：2015-12-08）

*通讯联系人